The Spectral Energy Distributions of Active Galactic Nuclei.

Belinda J. Wilkes

Smithsonian Astrophysical Observatory, 60 Garden St., Cambridge, MA 02138

Abstract. Key to our understanding of the workings of the most powerful energy sources in the universe, active galactic nuclei (AGN), are full, multi-wavelength observations of their emission. In this article the current observational status of AGN spectral energy distributions (SEDs) throughout the radio–γ-ray spectral regions is reviewed along with our intepretation of them and discussion of key areas which remain insufficiently explored.

The past decade has seen great strides in a number of spectral regions including: X-ray, γ-ray, infrared (IR), mm; and has resulted in observed SEDs for a larger and more representative fraction of the AGN population. This has led to a, sometimes reluctant, concensus on the important energy generation mechanisms in the various wavelength bands. However there are key spectral regions which remain beyond our observational capabilities, the EUV in particular, and regions where the full potential of current instrumentation has not yet been achieved, far-infrared and mm.

The inter-relation between the emission in the various spectral bands is discussed along with currently popular scenarios to explain both these relations and the SEDs in general. This is followed by a discussion of the role of dust and related emission line studies as well as the newly recognised class of NLSy1 galaxies. The article concludes with the suggestion, based on the results in a number of widely different studies discussed here, that orientation may play an important role in determing the observed properties of AGN with the pole-on view being provided by NLSy1 galaxies.

1. Introduction

Quasars and Seyfert 1 (Sy1) galaxies, their lower-luminosity siblings, (AGN is used to refer to quasars and Sy1 galaxies hereafter) are multi-wavelength emitters, with roughly equal energy output extending from the far-infrared (FIR) through to the X-ray region in all AGN, with extensions to radio and/or high energy γ-rays in $\sim$ 10%. Technological advances, particularly in the infrared (IR), mm, X-ray and γ-ray regions, have led to a dramatic increase in multi-wavelength observations of AGN over the past decade or so. This, in turn, has led to fundamental improvements in our understanding of the energy generation mechanisms at work in these powerful objects. This paper reviews the current

status of our observational knowledge and the energy generation mechanisms responsible for what we see.

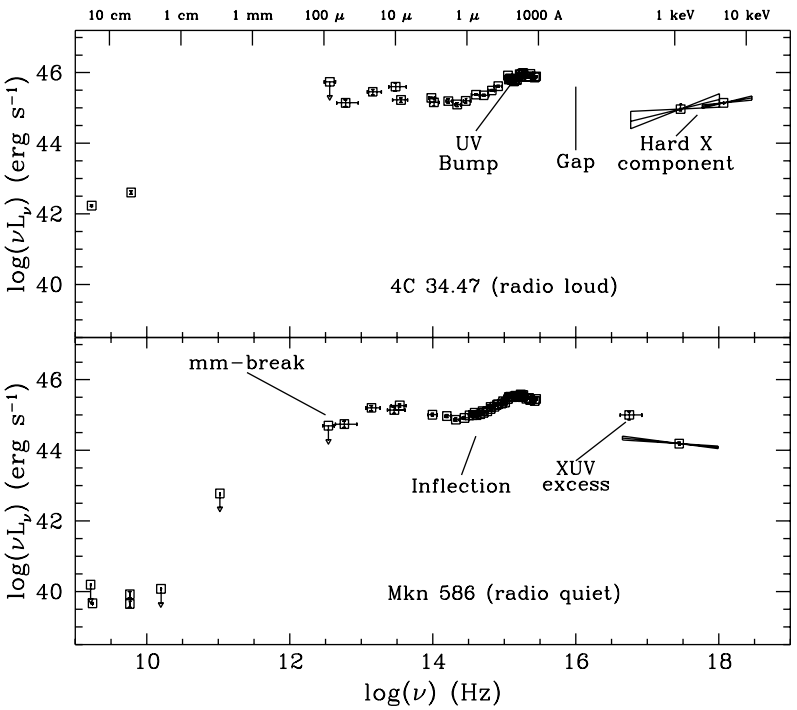

Figure 1. Rest-frame radio–X-ray spectral energy distributions (SEDs) for low-redshift radio-loud (upper) and radio-quiet (lower) quasars (from EWM94, their Figure 1). These are typical of the quality of SEDs in the current literature. The display of νL_ν vs ν shows the energy output as well as highlighting the structure of the SED.

2. Observational Status.

AGN emit roughly equal amounts of energy throughout the major part of the electromagnetic spectrum, extending from $> 100\mu$m in the FIR to > 10 keV in the hard X-ray. Roughly 10% also emit strongly at radio wavelengths and a significant fraction of these are strong γ-ray sources. Thus, to obtain a complete picture of these powerful sources, observations must be made at all wavelengths. To fully observe a single AGN requires obtaining time and observing on many different telescopes and satellites, often using more than one instrument in each case. In many parts of the spectrum these objects are sufficiently faint to push the limits of current technology. Given that many of them are variable on fairly short timescales, obtaining a single snapshot of a AGN SED is a daunting task and one that has not been completed for many AGN to date.

The number of compiled AGN SEDs in the literature has increased rapidly in the past decade, including many for individual objects (eg. Treves *et al.* 1988, Kolman *et al.* 1991, Kuhn *et al.* 1995, Puchnarewicz *et al.* 1995) and larger compilations at both low-redshift (Kriss 1988, Sanders *et al.* 1989, Barvainis 1990, Masnou *et al.* 1992, Elvis *et al.* 1994 (EWM94), Fiore *et al.* 1995, Laor *et al.* 1997) and higher redshift (Bechtold *et al.* 1994, Tripp, Bechtold & Green 1994). While many of these incorporate data observed over many years and often by many different groups in order to produce an SED, the majority are partially contemporaneous and provide a reasonable approximation to an instantaneous SED for relatively non-variable (ts $\lesssim$ 1 year) objects in at least the near-IR–optical range. When multiple epochs are available, it is also possible to estimate the level of variability and thus the uncertainty in the final SED. Examples of typical SEDs in the literature are given in Figure 1.

A small number of AGN known to be strongly variable have been the subjects of coordinated campaigns to monitor and relate their variability at a number of wavelengths simultaneously. The AGN which has the most complete, simultaneous coverage is the brightest nearby quasar: 3C273 (Tuerler *et al.* 1998, Courvoisier 1998) for which fairly complete SEDs are available at a number of epochs.

There remain parts of the SED which are not well-observed in more than a handful of objects. The FIR and sub-mm have very limited data which recent new capabilities, such as the photometer on the Infrared Space Observatory (ISO) and SCUBA (Submm Common-User Bolometer Array) on the James Clerk Maxwell Telescope (JCMT), should begin to rectify over the next few years. The extreme ultra-violet (EUV) region was observed by the wide field camera (WFC) on ROSAT and by the Extreme UV Explorer (EUVE) but only a handful of the brightest, low-redshift sources have been detected. In the γ-ray, the Gamma-Ray Observatory (GRO) has made an industry of observing core-dominated, radio-loud quasars (Fichtel *et al.* 1994). The lack of strong γ-ray emission from other classes of AGN implies that beaming is an important factor and results in a lack of knowledge on γ-ray emission from the general AGN population. In the high-energy γ-ray, only three BL Lac objects (e.g. MKN421, Zweerink *et al.* 1997, MKN501, Catanese *et al.* 1997) have been detected to date, two of which show flaring behaviour.

The radio region is also relatively unknown for radio-quiet AGN, which represent 90% of the class. This situation is rapidly improving as deeper surveys (FIRST: Gregg *et al.* 1996, NVSS: Condon *et al.* 1998) and directed studies (Kukula *et al.* 1998, Blundell & Beasley 1998) are completed.

3. Features of AGN Spectral Energy Distributions (SEDs).

The notable, standard features in quasar SEDs are labelled in Figure 1. Both radio-loud (RLQs) and radio-quiet quasars (RQQs) typically show bumps in the optical-UV and in the IR with an inflection point at $\sim 1\mu$m between the two. This inflection point, which represents a minimum in the energy output of the quasar, lines up with the peak in the starlight contribution from the host galaxy. In the lower luminosity, Seyfert galaxies the host galaxy contribution becomes comparable to the emission from the active nucleus, flattening the optical-IR

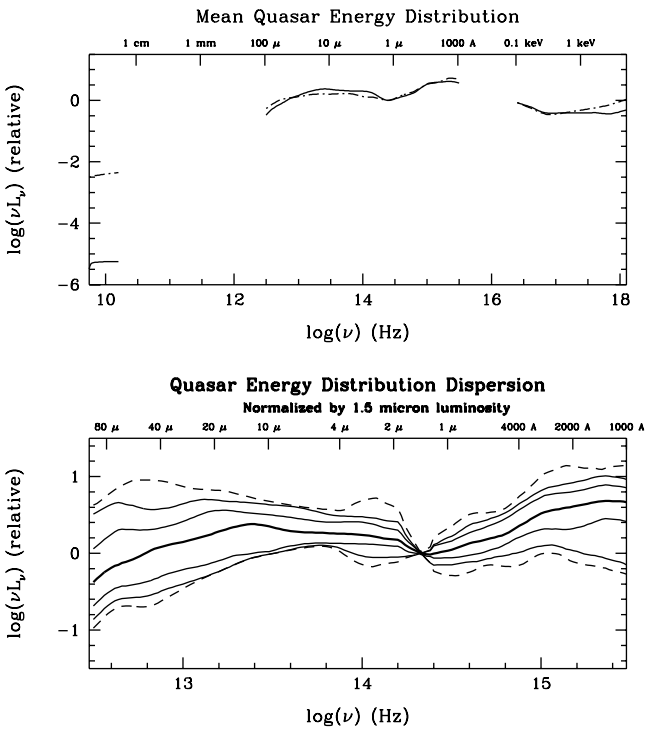

Figure 2. The upper plot shows the mean radio–soft X-ray spectral energy distribution for radio-loud (dashed) and radio-quiet (solid) low-redshift quasars. The lower plot shows the 68, 90 and 100 (dashed) Kaplan-Meier percentile envelopes showing the large dispersion around the median in the near-IR–UV region (from EWM94, their Figure 11).

SED and resulting in an apparent decrease in the strength of the optical and IR bumps. The dominance of the host galaxy emission $\sim 1\mu$m in these objects has been exploited to study their host galaxies (McLeod & Rieke 1994 a,b, Taylor *et al.* 1996, Dunlop *et al.* 1993).

Figure 2 shows the median SED for RLQs (dashed) and RQQs (solid) from EWM94 showing the remarkable similarity in the IR–UV region. A similar figure was presented by Sanders *et al.* (1989) for the PG quasar sample. Although these medians look very similar and well-behaved, there is a large dispersion around the median which fills most/all of the available parameter space (Figure 2, lower plot). This dispersion exacerbates searches for systematic dependencies of the SEDs on other quasar properties (luminosity, Wilkes *et al.* 1999) and needs to be included in any interpretation and modelling of the SEDs.

3.1. Infra-red and radio

The near-IR bump generally peaks $\sim 25 - 60\mu$m. It is broad, decreasing slowly to $> 100\mu$m, the longest wavelength accessible to IRAS. New observations by ISO should extend this coverage to 200 μm, but problems with the calibration have so far prevented reliable results. A recent paper from the ISOPHOT team

which reports far-IR SEDs for 10 RLQs and RQQs suggests that this situation will soon improve (Haas *et al.* 1998).

For RQQs, those objects with sub-mm or mm data are those which are brightest in the FIR and are mostly at low redshift. Typically very sharp cut-offs are seen between 100μm and 1 mm (Chini *et al.* 1989, Lawrence *et al.* 1991, Barvainis, Antonucci & Coleman 1992, Hughes *et al.* 1993). An example is shown in Figure 3.

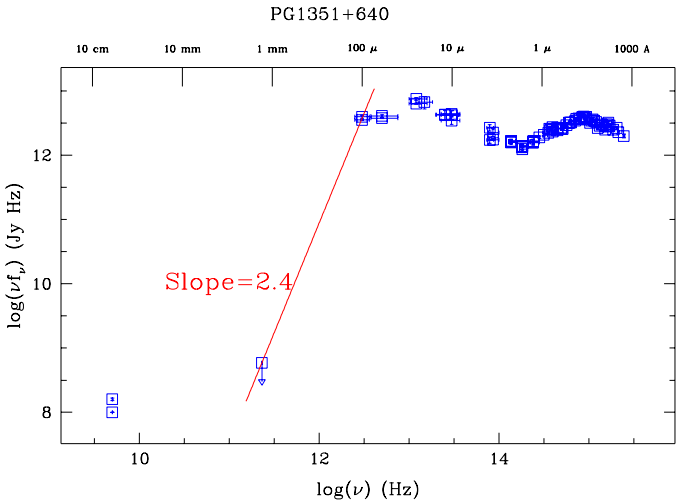

Figure 3. The radio–UV SED of the radio-quiet quasar, PG1351+640. The combination of the FIR flux from IRAS and the mm upper limit yeild an estimate for $\alpha_{fir} > 2.4$ ($f_\nu \propto \nu^{-\alpha_{fir}}$), close to the limit for a pure, homogeneous synchrotron source and so favoring thermal, dust emission in the far-IR.

RLQs fall into two distinct groups generally believed to be distinguished by the orientation of the source to our line-of-sight. Core-dominated (CD) RLQs are those in which relativistically beamed, synchrotron emission is pointed directly at us and so is boosted. In these sources, the radio–IR SED tends to be smooth, suggesting that the IR is a higher-energy extension of the synchrotron emission in the radio. In Figure 4 the mean SED of CDRLQ 3C273 from the compilation of 30 years of multi-wavelength monitoring by Tuerler *et al.* (1998) is displayed. The SED extrapolates smoothly from the radio into the IR and is observed to vary in a coordinated manner (Courvoisier 1998), strongly arguing for non-thermal emission throughout the radio–mid-IR SED. In the near-IR, $\sim 3\mu$m, there is a narrow peak of emission which does not vary in the same way and is believed to originate in hot dust (Courvoisier 1998). Even in this well-established, non-thermal source, dust emission is an important contributor.

Lobe-dominated (LD) RLQs are dominated by extended emission on either side of the central AGN, powered by the relativistic jets which, in these sources, are not close to our line-of-sight. Studies of the radio–FIR SEDs of the core emission have revealed a discontinuity in the mm region which implies that

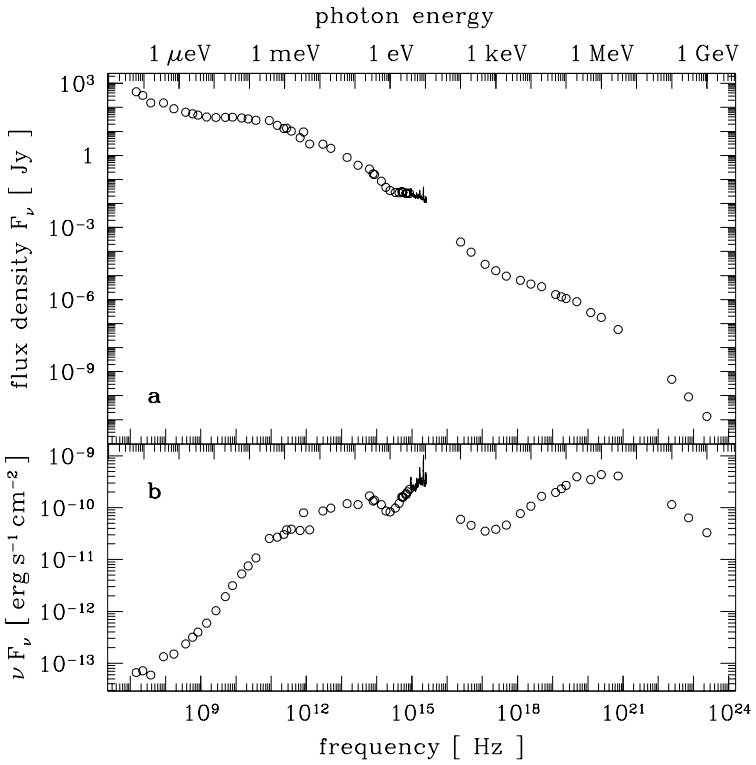

Figure 4. The average radio–γ-ray SED of the core-dominated, radio-loud quasar 3C273 shown as **a**: log(F_ν) and **b**: log(ν F_ν) vs log(ν) (from Tuerler *et al.* 1998, their Figure 6). The smooth extrapolation of the SED from radio into IR combined with correlated variability throughout the radio–mid-IR, strongly argue for a common/related, non-thermal emission mechanism in this spectral region.

emission in the FIR is unrelated to the non-thermal radio emission (Antonucci, Barvainis & Alloin 1990) and so favors a thermal origin for the FIR.

The radio properties of RQQs are typically either unresolved or with double, triple or linear structure providing strong evidence for jet-producing central engines similar to those in RLQs (Section 4.1.).

3.2. Optical and Ultra-violet

There is a second "bump" in typical quasar SEDs, the big blue bump (BBB), which dominates the optical-UV emission and often their total energy output. Since the X-ray emission is generally below an extrapolation of this BBB, it is generally thought to peak in the EUV region. Recent, high-quality, UV data (Figure 5, Zheng *et al.* 1997) shows evidence for a peak in the far-UV in low-redshift objects. The detection of a peak is a major step forward as it allows constraints to be placed on the EUV emission, which is the source of most of the ionising photons, and on the relation between the UV and soft X-ray

emission. At high redshift a similar measurement is difficult due to the affects of intervening absorption on the continuum shortward of the Lyα emission line.

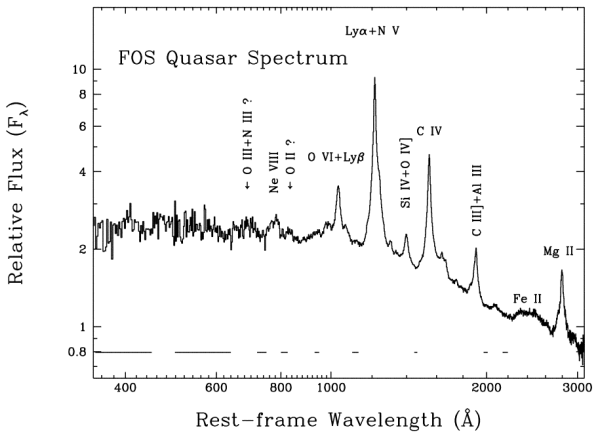

Figure 5. The composite of 284 HST FOS spectra of 101 AGN (from Zheng *et al.* 1997, their Figure 5), showing a clear change in the continuum slope consistent with a peak $\sim$ 1050Å.

3.3. X-ray and γ-ray

There are several components to the X-ray emission from AGN and their relative contributions differ depending on the type of object and energy range.

In RQQs and Sy1 galaxies, the mid-X-ray region ($\sim 1-5$ keV) is dominated by a power law with a slope $\alpha_x \sim 1$ ($F_\nu \propto \nu^{-\alpha_x}$, Wilkes & Elvis 1987, Reeves *et al.* 1997). In the same spectral region, CDRLQs tend to have stronger emission (Zamorani *et al.* 1981) and flatter slopes, $\alpha_x \sim 0.5$, while LDRLQs are intermediate between the two (Figure 6, Shastri *et al.* 1993, Reeves *et al.* 1997, Cappi *et al.* 1997).

Although the slopes generally steepen towards lower energies (0.1–2 keV, ROSAT band), RLQs remain relatively flatter than RQQs (Laor *et al.* 1997). These authors also suggest that this spectral difference may be linked to the width of the broad H$\beta\lambda$4861 emission line rather than the radio emission.

At harder X-ray energies, $\gtrsim$5 keV, the spectrum flattens, particularly in low-luminosity objects. This feature, first reported by Pounds *et al.* (1990), resulted in an apparent discrepancy between the low-energy (0.1–3.5 keV) *Einstein* slopes (Wilkes & Elvis 1987) and those measured by EXOSAT over the harder, 2–10 keV, energy range (Turner & Pounds 1989). This flattening is generally weak or absent in higher luminosity quasars (Williams *et al.* 1992, Lawson & Turner 1997). GRO OSSE observations show that the hard X-ray continuum of Sy1s generally extends to $\gtrsim$200 keV (Gondek *et al.* 1996, Zdziarski *et al.* 1994) before a high energy cut-off occurs.

A fluorescent, Fe Kα emission line is commonly observed, again tending to be stronger in low luminosity sources (Nandra *et al.*1997a,b). This Fe Kα line is often broad, and sometimes double-peaked. consistent with its origin in an accretion disk and, if so, providing the only direct observations of this

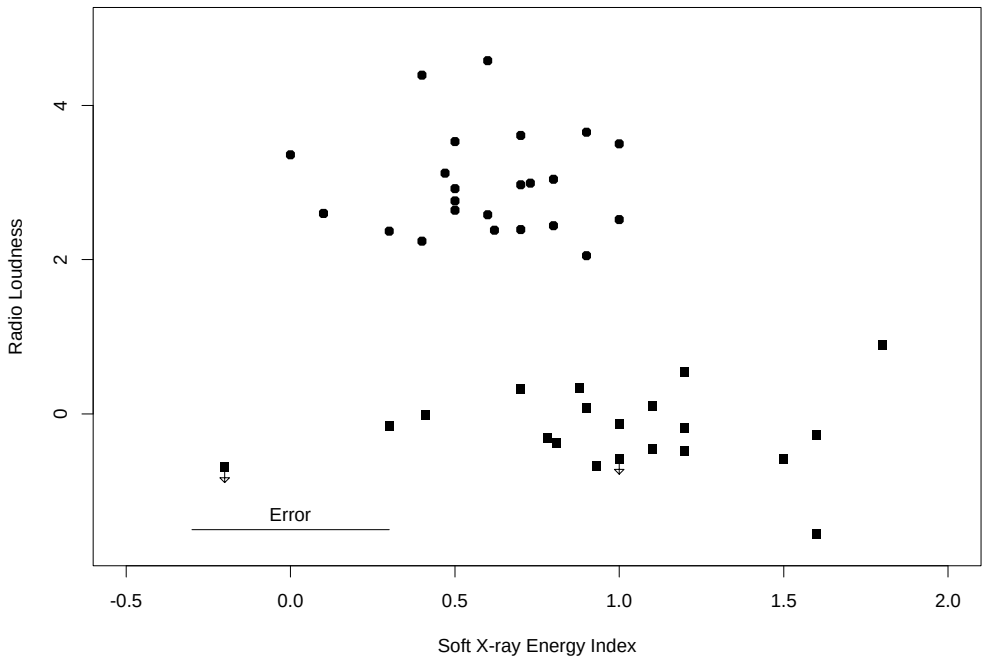

Figure 6. The relation between radio loudness and the *Einstein* soft X-ray slope (α_x, $F_\nu \propto \nu^{-\alpha_x}$) in quasars showing the systematically flatter slopes for RLQs (filled circles) in comparison with RQQs (filled squares) (data from Shastri *et al.* 1993).

accretion disk to date (Tanaka *et al.* 1995, George & Fabian 1991, Nandra these proceedings).

At soft energies, $\lesssim 1$ keV, the X-ray spectra of $\sim 50\%$ of both radio-loud and radio-quiet AGN steepens significantly to form the soft excess (Masnou *et al.* 1992). This component generally dominates their ROSAT (0.1–2 keV) spectra leading to systematically steeper slopes at these energies (Fiore *et al.* 1994, Buehler *et al.* 1995). The soft excess can be extremely steep and is often called the ultra-soft excess (Puchnarewicz *et al.* 1992, Boller, Brandt & Fink 1996). Given the general increase of both the BBB on the low energy and the ultra-soft excess on the high energy side of the EUV region, it is tempting to identify both as part of the same, BBB component. There is little direct evidence to this effect, for example observations of coordinated variability, but circumstantial evidence includes the anti-correlation of optical and soft X-ray slopes (Puchnarewicz *et al.* 1996) and the extrapolation of the soft X-ray into the UV region (Laor *et al.* 1997).

Studies of X-ray slopes as a function of redshift show changes which correspond well to these various components moving through the observed band as the redshift increases. Comparison of the slopes using a constant intrinsic energy range shows no dependence of α_x on redshift (Elvis *et al.* 1994, Cappi *et al.* 1997).

Another key component of X-ray spectra of quasars and Sy galaxies is absorption by cold and/or warm material. Sy1 galaxies and quasars typically show low absorption column densities ($N_H \sim 10^{20-21}$ cm^{-2}) often including ionised absorption edges indicating the presence of warm material (Halpern 1984). This warm material has been suggested to originate in the same material as that responsible for the narrow associated UV absorption lines common in many types of AGN (Mathur, Elvis & Wilkes 1995 and references therein).

4. Discussion.

4.1. The Radio–Infrared Connection

The only class of AGN for which the IR and radio emission appear to be directly related is the CDRLQs. The smooth extrapolation of their SEDs between the two regions supports the generally accepted scenario (Barthel, these proceedings) that they are dominated by non-thermal, synchrotron emission. This emission is beamed towards us and its intensity is relativistically boosted and so dominates the radio–near-IR emission. We note however that, even in these objects, dust emission can be significant in parts of the SED (eg. in 3C273 $\sim 3\mu$m, Courvoisier 1998).

One remaining puzzle in this apparently clear picture is that the non-thermal emission in RLQs has a very similar strength and shape to the IR emission from other AGN (Sanders *et al.* 1989, EWM94). The SED comparisons which have demonstrated this similarity of AGN SEDs across radio class have not distinguished between CDRLQs and LDRLQs, combining both types in generating the RLQ SED. However, unlike LDRLQs, CDRLQs possess many blazar-like qualities such as high polarisation and rapid coordinated variability, but also have a BBB and strong emission lines. Wills *et al.* (1992) concluded on the basis of polarisation studies, that CDRLQs are essentially the same as highly polarised quasars (HPQs). The SEDs of blazars, the rather heteregeneous class of objects including BL Lac objects, HPQs and optically violently variable sources (OVVs), are demonstrably different, primarily due to the lack of any BBB (Sanders *et al.* 1989, Impey & Neugebauer 1988). Their generally smooth SEDs and the higher incidence of detected variability in the IR has definitively established them as non-thermal sources (Impey & Neugebauer 1988). LDRLQs and RQQs, on the other hand, both show strong, broad and generally non-variable IR continua (Cutri *et al.* 1985, Edelson & Malkan 1987) with a steep cut-off in the FIR which does not extrapolate into the radio (Section 3.1.). This argues against the same, non-thermal emission component being responsible for both radio and IR emission. Initial ISO studies (Haas *et al.* 1998) suggest that CDRLQs are indeed non-thermal sources with blazar-like SEDs while LDRLQs have contributions from both thermal and non-thermal components. However this sample is small (10 objects) and a definitive solution to this puzzle awaits a systematic comparison of the SEDs of CDRLQs and "normal" AGN and/or LDRLQs.

There is a well-established, strong, $\sim$ linear relation between radio and IR emission in normal and starburst galaxies (Mas-Hesse 1992 and references therein) which is generally interpreted as a combination of thermal emission from dust heated by star formation and non-thermal emission from supernova

remnants. Radio studies of Seyfert 1 galaxies and RQQs, while showing extended structure reminiscent of star formation, also show central structures very similar to, but with lower luminosity than those in RLQs (e.g. De Bruyn & Wilson 1976, Ulvestad & Wilson 1984, Kukula *et al.* 1995, 1998, Blundell & Beasley 1998). This emission is too strong to be accounted for by normal star-formation rates (Ulvestad 1982) although these objects do fall on an extrapolation of the FIR-radio correlation (Kukula *et al.* 1998). This dichotomy can be explained by the large amount of scatter in the relation, which can hide and may be caused by significant contributions from unresolved, AGN-related emission. In addition, Kukula *et al.* (1998) argue that a correlation between the radio and optical AGN continuum would result in a AGN staying on the FIR-radio relation as the optical continuum heats the dust which emits the IR continuum. Note though that the existence of such a radio vs. optical relation is not clear (Lonsdale, Smith & Lonsdale 1995, Giuliano, Dario & Mezzetti 1996). Thus we conclude that the placement of AGN on the radio–IR relation does not prove that they are powered exclusively by a starburts.

4.2. The Infrared Emission: Thermal or Non-thermal

The typical steepness of the FIR cut-off, $\alpha_{fir} \sim 3.75 \pm 0.48$ (Hughes *et al.* 1993) in RQQs, provides a convincing argument for thermal emission from cool dust to dominate the FIR SEDs. Non-thermal, synchrotron emission, even from a single, homogeneous component, cannot produce a slope, $\alpha_{fir} > 2.5$ and more typical values from known synchrotron sources is $\alpha_{fir} \lesssim 1$ (Peacock & Wall 1982, Gear *et al.* 1994). Dust, on the other hand, can produce slopes as steep as 2–4, depending on the emissivity law adopted (Hughes *et al.* 1993).

The first strong evidence for cool dust emission at long wavelengths coincided with reports of host dust in Fairall 9 deduced from an observed delay between the optical and near-IR light curves of 400±100 days (Clavel, Wamsteker & Glass 1989). Detailed modelling of the dust reverberation deduces that the clouds are $\sim 0.3 - 1.3$ light years from the central source with dust sublimation temperatures 1300-2000K (Barvainis 1992). In addition the first large compilations of AGN SEDs (Kriss 1988, Sanders *et al.* 1989) demonstrated the ∼universal presence of an inflection at $\sim 1\mu$m. In a dust scenario, the corresponding decrease in the NIR emission coincides with the sublimation temperature. This mounting evidence for thermal dust emission led to the development of pure dust models to explain the IR continuum of AGN (eg. Sanders *et al.* 1989, Lawrence *et al.* 1991, Barvainis 1990, Pier & Krolik 1993, Rowan-Robinson 1995). These models generally include some combination of cool dust from the host galaxy, warm dust in star formation regions and hot dust, for example in a dusty torus, heated by the central ionising continuum. The remaining emission at 1 μm is assumed to originate in starlight from the host galaxy and perhaps a nuclear starburst in the higher luminosity objects (Lawrence *et al.* 1991). Problems with these models include: the lack of observed silicate features in the NIR spectra of AGN which results in the need to minimize their strength in models (Roche *et al.* 1984), the fine tuning required to explain the strong IR–X-ray correlation (Carleton *et al.* 1987, Brissenden 1989, Figure 7 from Green, Anderson & Ward 1992), and the similarity of the IR continua in RLQs and RQQs which, in this scenario, originate in different mechanisms. Although we noted

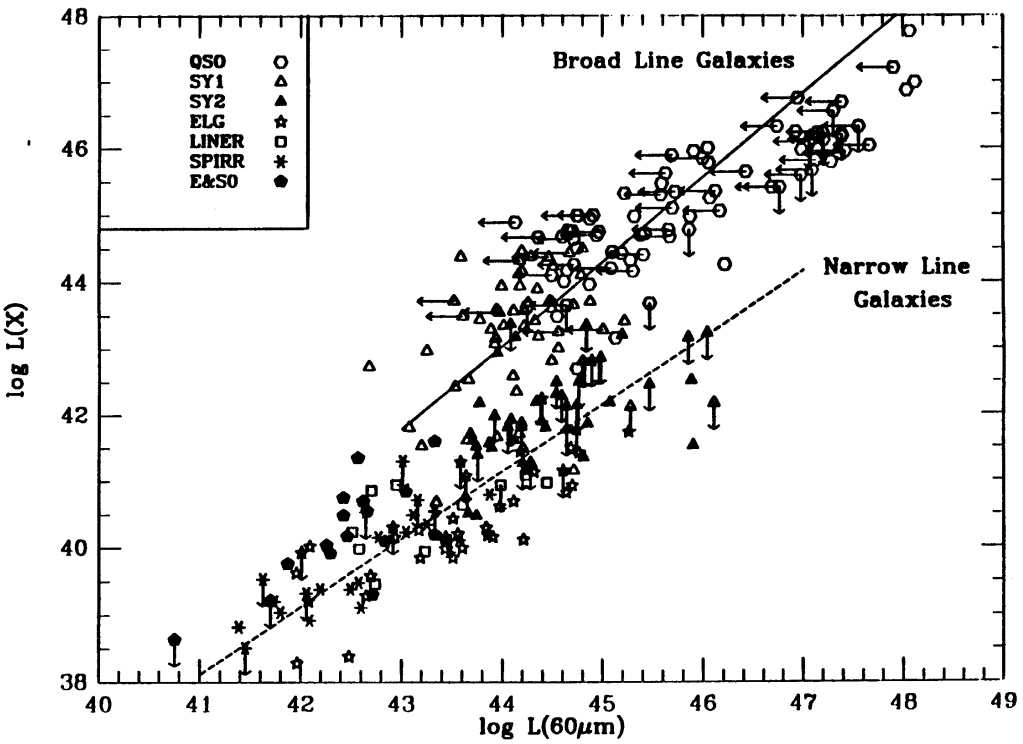

Figure 7. The IR vs X-ray luminosities of narrow and broad lined AGN (from Green, Anderson & Ward 1992, their Figure 2) showing the similar but shifted relation for the two types. This is interpreted as due to the increased importance of non-thermal IR emission in the broad-lined objects.

above (Section 4.1.) that this SED similarity may be the result of the inadequate samples studied to date.

The alternative of non-thermal, synchrotron emission in the IR is also discussed by many authors. The general lack of IR variability (Cutri *et al.* 1985, Edelson & Malkan 1987) and polarisation results in no direct evidence for the presence of non-thermal emission. It is also clear from the "bumpy" shape of the IR SED that dust is an important contributor. However the IR–X-ray correlation (Figure 7), the need for an underlying power law in accretion disk (AD) models for the BBB (Section 4.3., Siemiginowska *et al.* 1995, Laor 1990) and the presence of emission in excess of the host galaxy in AGN with no BBB (McDowell *et al.* 1989, Puchnarewicz *et al.* 1995) all argue in favor of a non-thermal component. While the steep FIR cutoffs observed in IR-bright RQQs clearly demonstrate the presence of cool dust, there remain similar observations which are inconclusive (Chini, Kreysa & Wargau 1997) and many types of RQQ which have not yet been observed. Recent results from long-term ($\sim$ 25 years) NIR monitoring of a subset of the optically-selected, PG quasars provide evidence for a level of variability similar to that reported in the optical plus correlated

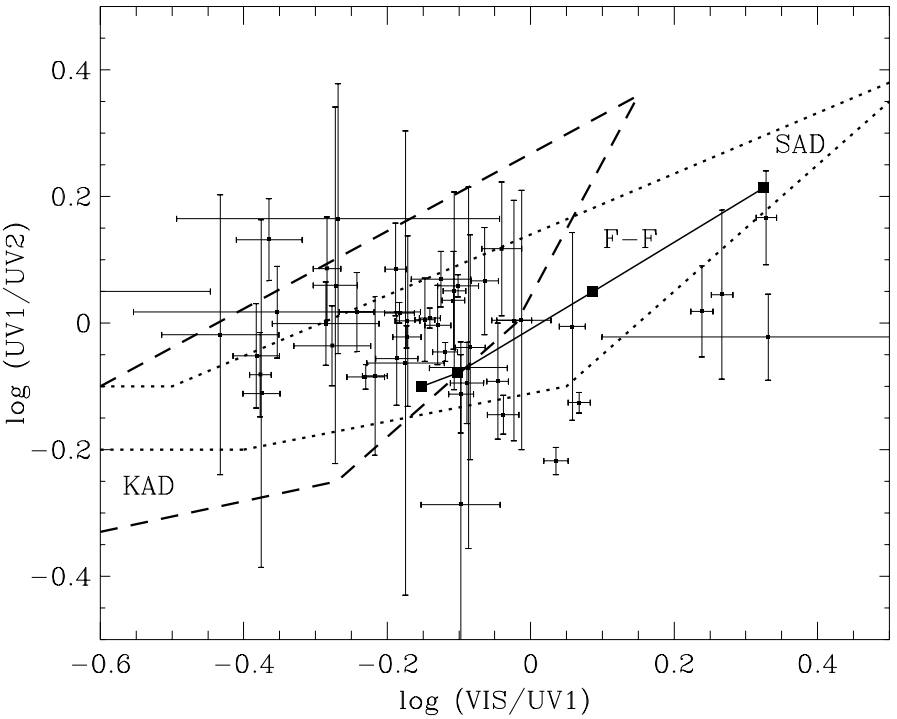

Figure 8. Color-color diagram of quasar SEDs compared with the locus of values predicted by both Kerr (KAD) and Schwarzschild (SAD) accretion disk models for the OUV BBB (from Siemiginowska *et al.* 1995, their Figure 7).

variations from 1–10 μm in at least one object. Both results are best explained in terms of non-thermal emission (Neugebauer 1996).

In conclusion, the interplay of non-thermal and thermal emission in the IR SEDs of AGN remains unclear. It is likely that both contribute to varying degrees and their relative dominance may be a systematic function of other properties such as the radio emission.

4.3. The Optical/Ultra-Violet Big Blue Bump

The origin of the BBB in AGN has been the subject of some debate in the literature over the past decade or so. Thermal emission from an optically thick, geometrically thin accretion disk (AD) is favored by many. Observationally, when combined with an underlying power law which contributes significantly at long wavelengths (5000Å– 1μm), it can re-produce the range of shapes observed for the OUV BBB (Figure 8, Siemiginowska *et al.* 1995). When combined with a corona, it is able to explain the ultra-soft X-ray excess as well (Czerny & Elvis 1987, Sun & Malkan 1989, Laor 1990, Siemiginowska *et al.* 1995). Theoretically, since AGN are generally believed to be powered by a central massive black hole, an AD is very likely to be present in an AGN core and to be a

substantial contributor to its energy output. However problems with this model occur when detailed predictions are compared with the observations. In particular, AD models generally predict that the emission is polarised and has Lyman edge absorption due to the large optical depths. Neither of these properties is universally present in AGN SEDs and there is an on-going debate concerning the importance of these discrepancies (Koratkar *et al.* 1995, Koratkar, Kinney & Bohlin 1992, Blaes & Agol 1996, Antonucci *et al.* 1996, Shields, Wobus & Husfeld 1998, Agol, Blaes & Ionescu-Zanetti 1998).

The main alternative model for the BBB is free-free emission (Barvainis 1993). This model can produce an OUV continuum with roughly the correct shape, but it is unable to explain the observed range of slopes (Siemiginowska *et al.* 1995). It is also inconsistent with the lack of observed, strong X-ray emission lines (Kriss 1994, Collin-Souffrin *et al.* 1996).

In conclusion, despite the continuing debate, the AD plus corona model remains the most viable model for the OUV–soft-X-ray BBB in AGN SEDs.

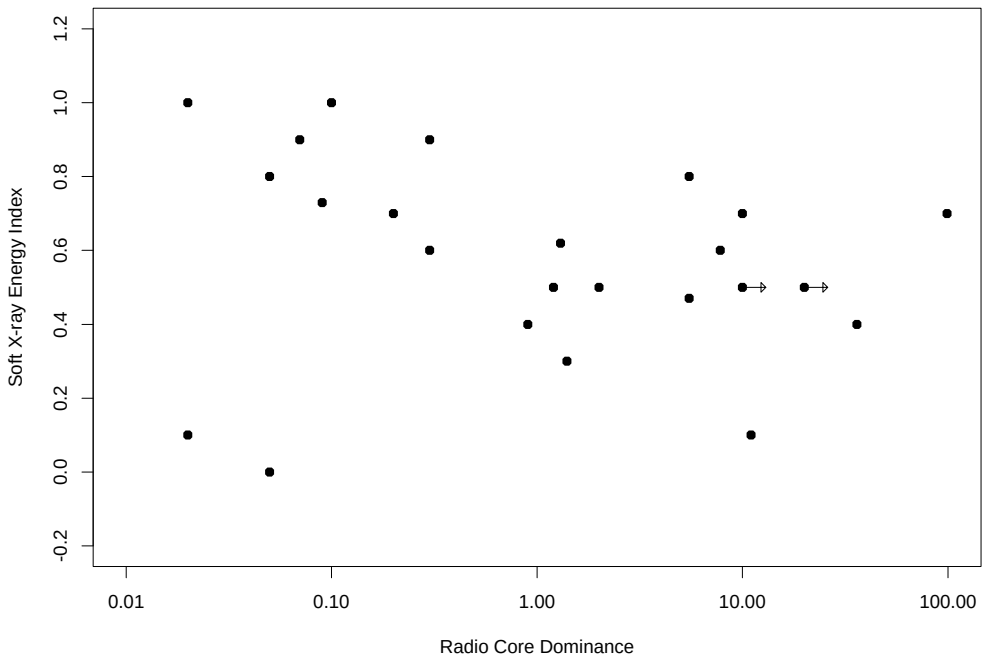

Figure 9. *Einstein* soft X-ray slope (α_x) as a function of radio core dominance (R) demonstrating that there is a strong correlation between the two with CDRLQs having significantly flatter slopes (data from Shastri *et al.* 1993). Two objects with very low values of R also have very flat X-ray slopes suggesting that, at the most edge-on inclinations, the steep spectrum X-ray component is occulted.

4.4. The X-ray Emission

The primary X-ray source in RQQs is responsible for generating emission with a power law slope, $\alpha_x \sim 1$ throughout most of the X-ray region ($\sim 1-$ >200 keV). The biggest problem faced by current models for the X-ray emission from AGN, is the origin of this primary emission. A non-thermal model with dominant pair production is ruled out in current data as it predicts a steepening of the spectrum at energies $\gtrsim$10 keV, contrary to the observations which typically show extensions out to >100 keV (Gondek *et al.* 1996, Zdziarski *et al.* 1994). The simplest, non-thermal models include a power-law distribution of electrons which Thomson scatter off soft seed photons. These models match the observed spectral slope but do not produce the observed $\sim$ 200 keV, high-energy cut-off (Gondek *et al.* 1996). Currently the best models include repeated Compton scattering, either combined with a non-thermal plasma having power law electron distribution or thermal Comptonisation of soft seed photons (Gondek *et al.* 1996, Zdziarski *et al.* 1996). The geometry of the source is not well-determined, a leading contender is the two-phase model of Haardt & Maraschi (1993, 1991) in which the X-rays are produced via inverse Compton scattering in a hot corona surrounding a cooler AD which is the main source of the UV seed photons. This model is successful in producing the average Sy1 spectrum including the high-energy roll-over and can produce somewhat steeper slopes, but is unable to produce the flatter slopes which have been observed in a few Sy1 galaxies (e.g. NGC 4151, Yaqoob, *et al.* 1993). A more recent update of this model involves blobs rather than a smooth corona and solves some of these problems (Haardt, Maraschi & Ghisellini 1994).

The flattening of the X-ray spectrum $\sim$5–10 keV (Section 3.3.) is widely accepted to originate in Compton reflection of the primary X-ray continuum in cool ($\sim 10^4$K), optically thick material at the surface of the AD (Guilbert & Rees 1988, Lightman & White 1988, Pounds *et al.* 1990, Nandra & Pounds 1994). Reflection from neutral and ionized material, probably located in the putative molecular torus and/or the AD, has now been observed in a large number of Sy1 galaxies (Fiore *et al.* 1992, Turner *et al.* 1997a, Reynolds 1997). This component dominates the X-ray spectrum up to $\sim$ 300 keV (Lightman & White 1988) where the material becomes optically thick to Compton scattering. The observed strength of the reflection component varies from object to object and tends be larger in lower luminosity sources (Williams *et al.* 1992, Lawson & Turner 1997).

The mid-X-ray continuum tends to be stronger and flatter in RLQs (Section 3.3.). This is thought to be due to a radio-linked, synchrotron self-Compton (SSC) component (Zamorani *et al.* 1981, Wilkes & Elvis 1987). A strong correlation is present between X-ray slope and the radio-core dominance (Figure 9), supporting an interpretation in which the flatter, $\alpha_x \sim 0.5$, SSC component is beamed and so stronger and more dominant in core-dominated sources (Shastri *et al.*1993, Lawson & Turner 1997).

4.5. X-ray Emission and Unification.

In the context of Sy1/Sy2 unification, Sy2s are believed to be edge-on Sy1 galaxies whose central regions are obscured by optically thick material, perhaps in a torus (Antonucci & Miller 1985). The hard X-ray emission of the two classes of

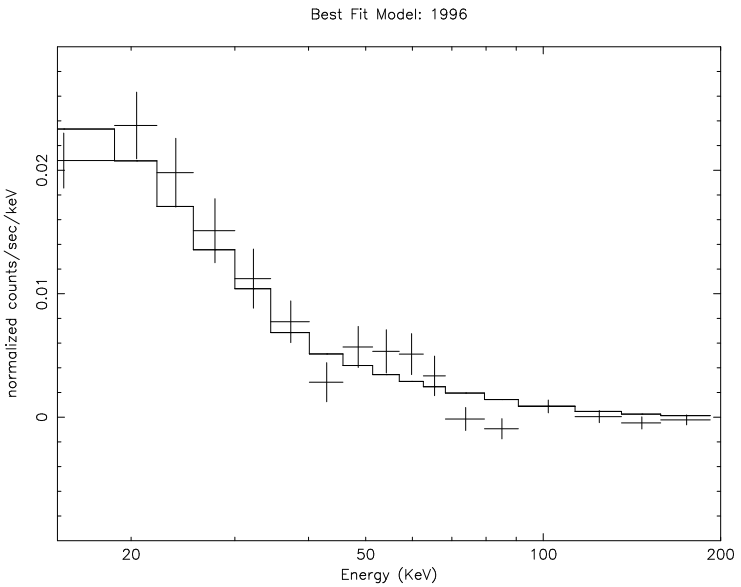

Figure 10. Hard X-ray (PDS) SAX spectrum of the Seyfert 2 galaxy ESO103-G35 (from Wilkes *et al.* 1998, their Figure 2).

source is expected to be similar since the column densities are sufficiently low that the hard X-rays are directly visible, even when viewed edge-on. Recent X-ray studies of Sy2 galaxies with *Ginga* (Smith & Done 1996) and ASCA (Turner *et al.* 1997b, Awaki 1997, Awaki *et al.* 1997) demonstrate that the 1–10 keV (1–18 keV for *Ginga*) are indeed similar, including contributions from a primary, $\alpha_x \sim 1$, power law, a reflected component and Fe Kα emission. BeppoSAX and RXTE (Rossi X-ray Timing Explorer) data, which extend to higher energies, confirm that the hard X-ray power law extends to $\gtrsim 50$ keV (Wilkes *et al.* 1998, Blanco 1998), again consistent with Sy1 galaxies (Figure 10). Thus the X-ray emission provides strong support for the unification of Sy1/Sy2 galaxies.

Again consistent with unification models, Sy2 galaxies generally show strong low-energy absorption with column densities $\gtrsim 10^{22}$ cm^{-2}, compared with $N_H \sim 10^{20-21}$ cm^{-2} for Seyfert 1 galaxies and quasars (Section 3.3.). These column densities are generally consistent with absorption in the obscuring material (Turner *et al.* 1997b, Awaki 1997).

4.6. The relation between X-ray and Optical Emission

There is a well-established correlation between X-ray and optical emission in AGN such that higher luminosity sources have relatively weak X-ray emission (Worrall *et al.* 1987, Wilkes *et al.* 1994, Green *et al.* 1995, Green, these proceedings). Similar evidence is found when comparing low and high luminosity quasar SEDs (Wilkes *et al.* 1999). The relation as determined by Wilkes *et al.* (1994) is:

$$< \alpha_{ox} >= (0.11 \pm 0.02)(log L_{opt} - 30.5) + (1.53 \pm 0.02) \qquad (1)$$

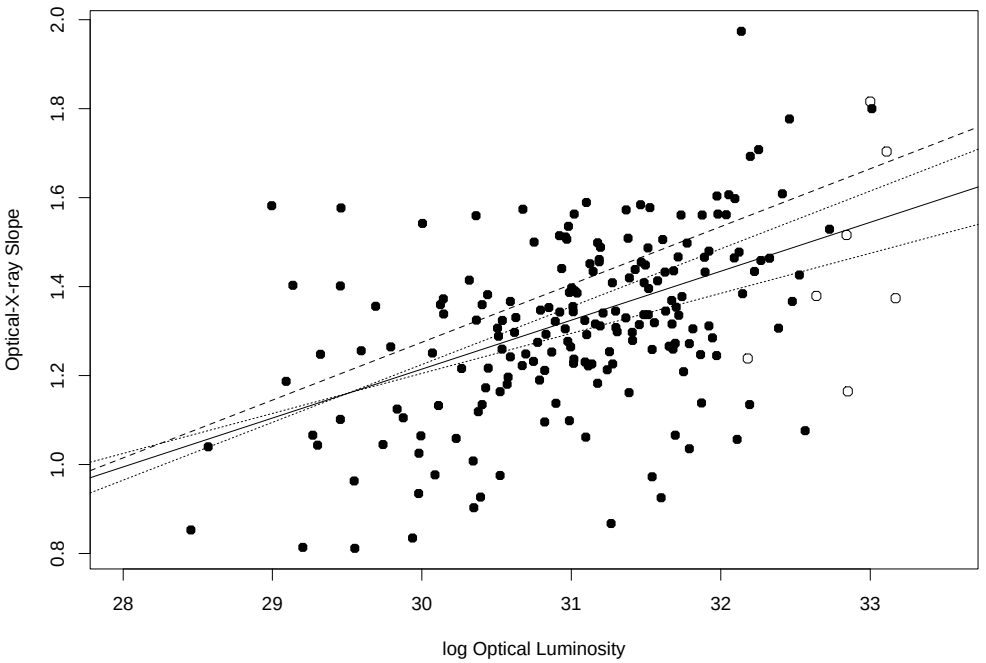

Figure 11. α_{ox} vs L_{opt} for the detected RLQs in the *Einstein* quasar sample of Wilkes *et al.* (1994, filled squares) and the ROSAT, high-redshift quasars of Bechtold *et al.* (1994, open circles, similar to Bechtold *et al.* 1994, Figure 4). Superposed are the relation for SSRLQs from Worrall *et al.* (1987, dashed line) and that for RLQs from Wilkes *et al.* (1994, solid line) with the 1σ error range indicated (dotted).

where α_{ox} is the effective optical-to-X-ray slope and L_{opt} the optical luminosity at 2500Å (Tananbaum *et al.* 1979).

The existence and behavior of an α_{ox} vs L_{opt} relation has been disputed by a number of authors. For example, ROSAT observations of high-redshift quasars suggest that it holds for RQQs only while for RLQs the relation flattens at high redshift (Bechtold *et al.* 1994). This conclusion was reached based on a comparison of ROSAT-observed, high redshift quasars with data from Wilkes *et al.* (1994) using the relation between α_{ox} and L_{opt} from the smaller sample of Worrall *et al.* (1987). This relation is determined using a sample of $<$ half the size and is consistent with equation (1) but not so well-constrained. In Figure 11 the X-ray detected RLQs from Wilkes *et al.* (1994) are shown (filled circles) with those from Bechtold *et al.* (1994, open circles). The dashed line indicates the Worrall *et al.* (1987) relation for steep-spectrum (SS) RLQs and suggests that the high-redshift ROSAT objects have systematically strong X-ray fluxes. However using the updated relation for RLQs determined from both detections and non-detections in the *Einstein* database, i.e. replacing the constant of 1.53 in equation (1) with 1.27 (from Figure 14b of Wilkes *et al.* 1994), the RLQ discrepancy at high-redshift is less convincing (solid line in Figure 11 with the 1σ error range shown dotted). Observations of more, high redshift quasars are needed to clarify any RLQ vs RQQ difference.

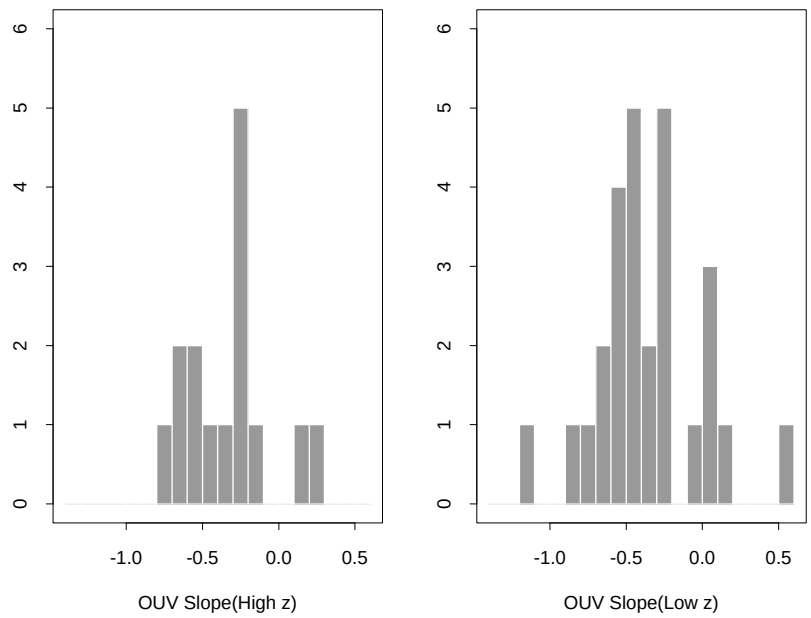

Figure 12. Comparison of the optical–UV slopes of high and low-redshift (z) samples of quasars matched in evolved luminosity (data taken from Kuhn 1996) demonstrating the lack of evolution in the continuum slope. This argues for a quasar population which is short-lived with multiple generations as opposed to a single-long-lived generation which would be expected to evolve as the central black hole accretes material.

La Franca *et al.* (1995) suggest that the relation is linear. This discrepancy may be due to their assumption that photometric errors dominate the dispersion in the relation whereas in reality the errors in L_{opt} are significantly smaller than the dispersion. Yuan, Siebert & Brinkmann (1998), on the other hand, suggest that the relation is an artifact caused by an intrinsic dispersion in L_{opt} which is ~ 5 times larger than that in L_X. However there is no apriori reason why this should be the case and there is no (other) evidence for such a difference in the intrinsic dispersion of the optical and X-ray luminosities.

In an extension to the α_{ox} vs L_{opt} relation Zheng & Malkan (1993) present evidence for a color-luminosity relation in AGN which is consistent with the BBB moving towards lower energies as the luminosity increases. This luminosity dependence of AGN SEDs can explain the Baldwin Effect in terms of the reduced ionising flux at high luminosity (Zheng & Malkan 1993). However, Kuhn (1996), in her comparison of high and low redshift quasar SED matched in evolved luminosity, sees no such evolution of the BBB (Figure 12). Kuhn (1996) suggests that the reason for the discrepancy is the lack of allowance for host galaxy emission in the Zheng & Malkan (1993) analysis. The weakening of the host galaxy contribution systematically steepens the BBB as the luminosity increases causing the observed increase in slope.

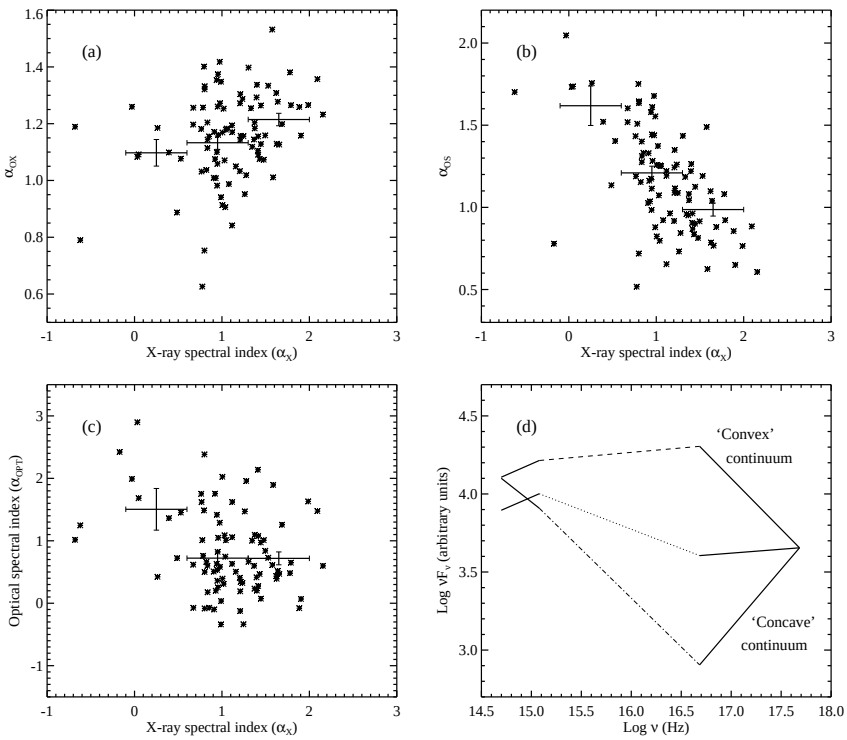

Figure 13. The inter-dependence of the optical and X-ray slopes in the X-ray selected RIXOS AGN sample. The strong anti-correlations of α_x with both α_{opt} and α_{os} (effective optical-to-soft-X-ray slope, 0.2 keV) combined with its correlation with α_{ox} lead to the schemmatic diagram showing the range of SEDs present in the sample (from Puchnarewicz *et al.* 1996, their Figure 9).

In summary, evidence to date supports the relative increase in the strength of the BBB implied by the α_{ox} vs L_{opt} relation but not a change in its shape. There is also no evidence for evolution of the optical–X-ray SED with redshift (Wilkes *et al.* 1994, Elvis *et al.* 1994). The luminosity dependence of the SED results in a decrease in the number of ionising photons which is likely to be an important contributor to the Baldwin effect, *i.e.* the constancy of the UV emission line fluxes with increasing luminosity (Mushotzky & Ferland 1984).

4.7. The Role of Dust in the OUV and X-ray

Over the past few years, evidence has been mounting which suggests that dust plays an important role in determining the wide dispersion in the SEDs of AGN. AGN are predominantly selected in optical surveys, commonly due to their UV excess in comparison with stars and galaxies (e.g. PG survey, Schmidt & Green 1983, LBQS survey, Hewett *et al.* 1995). This results in a strong bias towards optically-bright sources. Radio surveys are largely free from this bias and have resulted in the detection of unusually red AGN (Smith & Spinrad 1980, Webster *et al.* 1995). This led to the suggestion that many existing surveys are missing a substantial fraction of the population by selecting against red objects. X-ray

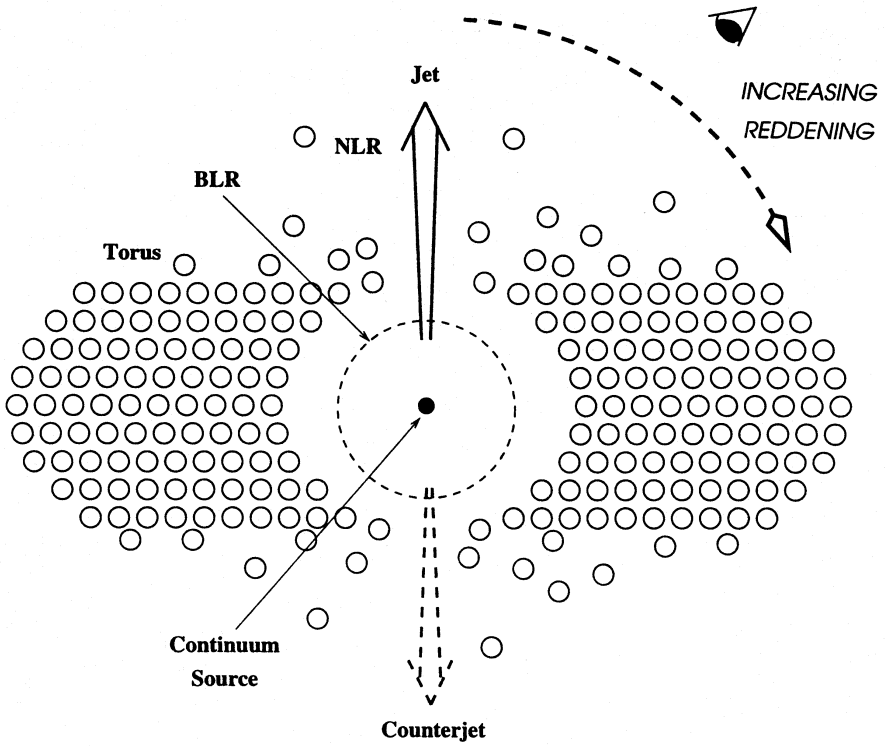

Figure 14. Schemmatic diagram of the central regions of an AGN showing an increasing column density of dust as the plane of the central AD is approached (from Baker 1997, her Figure 19).

surveys avoiding the soft X-ray band, which is strongly affected by absorption, should also be relatively unaffected by this bias. Evidence for a wider range of optical continuum slopes in the AGN population varies from sample to sample. The X-ray surveys: Cambridge-Cambridge ROSAT Serendipity Survey (CCRSS, Boyle, Wilkes & Elvis 1997) and ROSAT deep (Shanks *et al.* 1991) show a range of slopes very similar to optical samples (Boyle & di Matteo 1995) while the ROSAT International X-ray/Optical Survey (RIXOS) and *Einstein* Medium Sensitivy Survey (EMSS) samples show a wider range (Puchnarewicz *et al.* 1996, Stocke *et al.* 1991). Part of this discrepancy may be explained by differing amounts of host galaxy contamination in the various samples but it is intriguing to note that the CCRSS and RIXOS are selected using essentially the same X-ray energy range. Laor *et al.* (1997) in a study of a subset of the optically selected PG sample argue that the redder objects in the RIXOS sample would have been seen if present in the PG sample. The debate continues as evidence mounts for the existence of red AGN in radio and X-ray selected samples (e.g. Kim & Elvis 1998, Becker *et al.* 1997, Masci, Drinkwater & Webster 1999). It is likely that hard X-ray selected samples from AXAF and XMM, using a sufficiently hard energy range to be relatively unaffected by absorption for column densities typical of those seen in red AGN, will obtain AGN samples representative of the true parent population and so be able to address the question of the dispersion in their SEDs.

The RIXOS sample of 108 AGN noted above is selected in the hard X-ray band of ROSAT (0.4–2.0 keV) to minimise the affect of soft X-ray absorption. Not only does this sample show a wide range in the OUV slope, but there is also an intriguing set of correlations between the optical and soft X-ray slopes (Puchnarewicz *et al.* 1996). These correlations show a reddening of the optical continuum when the X-ray spectrum becomes harder (Figure 13). This implies that absorption by dusty material is responsible for both and the authors suggest that the wide range of optical continuum slopes is due to a range in the amount of dust redenning. In their much smaller (23 objects) subset of the optically selected PG sample, Laor *et al.* (1997) also find a positive correlation of the X-ray slope with α_{ox} which they interpret as a decrease in the strength of the hard component.

In RLQs, Baker (1997) and Baker & Hunstead (1995) show a strong correlation of the equivalent width (EW) of [OII]λ3727 with the radio core dominance, R, which suggests a strong orientation dependence of the optical continuum since [OII] is generally throught to be emitted isotropically. [OIII]λ5007 has a weaker dependence on R (see also Jackson & Browne 1991) and the ratio of [OII] to [OIII] depends on R. These correlations can be explained by an orientation dependence of [OIII] which is similar to, but not as strong as, that of the optical continuum, weakening the orientation dependence of the EW for this line. Since the Balmer decrement is also observed to be a strong function of R (Baker 1997, Jackson & Browne 1991), these relations are interpreted as due to an increasing column density of dust as the line-of-sight progresses from pole-on to edge-on in RLQs. The optical continuum originates in the smallest region and so would be most affected by the absorption while the [OII], largely emitted at greater distances from the central source than the dust, would be the least affected (Figure 14).

4.8. Where do the NLSy1s fit in?

The properties of NLSy1 galaxies are discussed by a number of other authors in these proceedings. As a reminder, their most notable properties (Table 1) are narrow (< 2000 km s^{-1}) broad emission lines, strong optical FeII emission, weak [OIII]λ5007 and very steep soft X-ray spectra. The SED of a NLSy1 showing the typically strong, hot BBB and steep soft X-ray slope is shown in Figure 15. Their properties place them at the extreme end of the "first eigen vector" of Boroson & Green (1992) which explains ~ 30 % of the scatter in the line continuum correlation of the PG sample (Boroson & Green 1992, Boller, Brandt & Fink 1996, Lawrence *et al.* 1997). Popular scenarios to explain this phenomenon include Eddington limited flow (Pounds, Done and Osborne 1995, Laor *et al.* 1997, Laor these proceedings) and/or a larger BLR, resulting in lower velocities and narrow lines, due to the strong, steep soft X-ray continuum (Wandel & Boller 1998, Wandel these procedings).

Another scenario which has been suggested but largely discounted in the past (Boroson & Green 1992, Boroson 1992) is one of orientation. The main argument against this scenario is based on the strong presence of the [OIII] line in the correlations. [OIII] was, until recently, thought to be orientation independent implying that orientation cannot be an important factor in eigen vector one. However, in the light of recent evidence for the orientation dependence of [OIII]

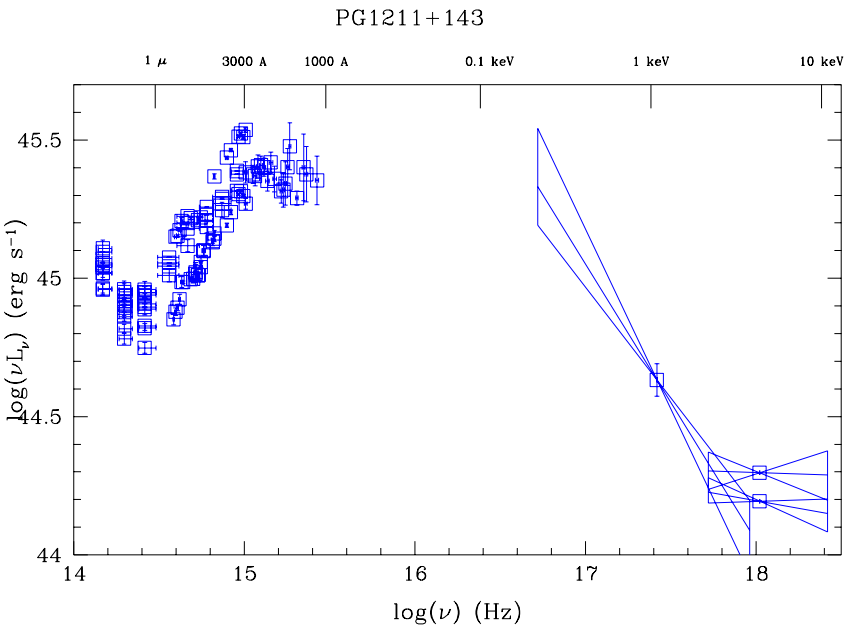

Figure 15. The rest-frame, near-IR–X-ray Spectral Energy Distribution (SED) of the NLSy1 galaxy PG1211+143 showing the unusually steep soft X-ray spectrum and a very pronounced OUV–soft-X-ray BBB which often characterises these sources (data from EWM94).

in RLQs (Section 4.7.), this argument weakens. Re-examination (below) of an orientation scenario suggests that it is at least as viable as those mentioned above and perhaps explains more of the observed properties.

It is well-established that RQQs have significantly stronger optical FeII emission than RLQs (Boroson & Green 1992, Bergeron & Kunth 1984). It is also generally accepted that CDRLQs have stronger optical FeII emission than LDRLQs (Shastri *et al.* 1993, Joly 1991, Boroson, Persson & Oke 1985, Peterson, Foltz & Byard 1981) although this has been disputed (Jackson & Browne 1991, Bergeron & Kunth 1984). Based on a tendency for edge-on LDRLQs to have broader H$\beta\lambda$ 4861 lines than face-on CDRLQs, Wills & Browne (1986) argued that the broad line widths are correlated with the orientation of the RLQs. Thus we see that the pole-on, CDRLQs have both narrower broad lines and stronger optical FeII emission than LDRLQs. If we draw an analogy between RLQs and RQQs, we find that NLSy1s are those Sy1s with the narrowest broad lines and the strongest optical FeII. For RQQs which, by definition, have no strong radio emission, there is no accepted orientation indicator with which to determine independently whether they are viewed pole-on. However, assuming that the Hβ line behaves similarly in RQQs and RLQs, we are led to the conclusion that NLSy1s are the pole-on RQQs.

Table 1. Characteristics of NLSy1 Galaxies.

Parameter	NLSy1	L$\sim$L$_{Edd}$	Large R$_{BLR}$	Pole-on Orientation
Reference		1,2	3	
Optical FeII	Strong	X	X	$\surd$
[OIII]	Weak	X	X	$\surd$
CIV,CIII]	Weak	X	X	$\surd$
FWHM(Hβ)	Narrow	$\surd$	$\surd$	$\surd$
α_x	Steep	$\surd$	$\surd$	$\surd$
X-ray Vbly	Strong	X	X	$\surd$
L$_X$(hard)	Weak	$\surd$	$\surd$	$\surd$
BBB	Strong	$\surd$	$\surd$	$\surd$
BBB	Hot	$\surd$	$\surd$	X

Reference:
1. Pounds, Done & Osborne 1995
2. Laor *et al.* 1997
3. Wandel & Boller 1998

The successes and failures of the various scenarios for NLSy1s are shown in Table 1. An orientation scenario with NLSy1s analogous to CDRLQs would explain the strong FeII and narrow Hβ properties as well as weak [OIII] and [OII] following Baker's results (Section 4.7.). Assuming an AD is the source of the ionising continuum, a pole-on AD would also yield weaker and unobscured hard X-ray emission, a stronger BBB and a stronger, hotter soft X-ray excess (Netzer, Laor & Gondhalekar 1992 and references therein). A clear view to the inner regions of the AD could also explain the larger observed incidence of soft X-ray variability in these sources since the inner regions have the smallest variability timescales. The high densities in the BLR of NLSy1s deduced from the weakness of CIVλ1549 and CIII]λ1909 (Kuraszkiewicz *et al.* 1998, Wilkes *et al.* 1999) could also be explained in terms of a clearer view to lower radii in the BLR. Orientation, while being the least exciting of the scenarios in Table 1 since it lacks any direct connection to or means to constrain the central engine, can explain more of the observed properties of NLSy1s than its two main rivals. The only property which remains unexplained is the relative weakness of the low temperature BBB emission which in some cases results in no observable BBB in the OUV at all (Puchnarewicz *et al.* 1995).

5. Conclusions and Questions

The spectral energy distributions (SEDs) of low-redshift (z) AGN are now fairly well-observed and understood throughout much of the electromagnetic spectrum. The dispersion around the median SED is large and needs to be addressed by models. Key regions which remain under-studied are the far-IR–submm, the EUV and the γ-ray. At higher redshift, samples remain small but are growing.

The main conclusions are:

- an optically thick, geometrically thin AD plus surrounding corona is the most viable model for the OUV BBB and ultra-soft X-ray excess components of AGN SEDs.

- cool dust dominates the far-IR continuum of RQQs and LDRLQs while CDRLQs are dominated by non-thermal, synchrotron emission.

- the X-ray spectrum is a combination of an underlying power law and reflection of this emission in the cool material at the surface of an AD. The amount of reflection occurring decreases with the luminosity of the source.

- there is significant evidence for an increase in the relative strength of the OUV BBB with luminosity.

Key open questions in the interpretation of AGN SEDs are:

1. **Are the radio–IR SEDs of CDRLQs and LDRLQs different?** This is expected if dust dominates the IR emission in LDRLQs and RQQs while the CDRLQs are non-thermal.

2. **What is the true range of SEDs in the AGN population?** The relatively unbiassed, hard-X-ray selected samples facilitated by the X-ray satellites AXAF (NASA) and XMM (ESA), both due for launch in 1999, provide the best opportunity for a relatively unbiassed sample. Radio samples are also relatively unbiassed but are largely confined to the radio-loud 10% of the population, which may introduce its own biasses. These samples would allow us to address the following questions:

   (a) **How important is dust attenuation to the observational properties of AGN?**

   (b) **How important is orientation to the observed properties of RQQs?** This question is probably linked to the last one since the distribution of attenuating material is likely to depend on the source orientation. The question may perhaps be addressed by further studying the NLSy1 objects and the possible role of orientation in explaining their properties.

3. **What is the interplay between thermal and non-thermal emission in the near and far-IR?** ISO may begin to address this question by observing the IR SEDs of the brightest sources but we will not be able to observe representative samples until SIRTF begins its operation $\sim$ 2002. IR variability studies also address this question and are becoming more possible as IR array technology advances.

4. **Does the SED evolve?** More SEDs for high redshift quasars are needed to address this question.

Acknowledgments. I would like to thank the conference organisers for inviting me to present this review and so forcing me to catch up with at least some of the recent literature. I am very grateful to my colleagues at SAO, in particular Martin Elvis, Paul Green, Eric Hooper, Joasia Kuraskewicz, Smita Mathur, Harvey Tananbaum and Marianne Vestergaard for many fruitful discussions. I acknowledge the financial support of NASA contract NAS8-39073 (AXAF Science Center).

References

Agol, E., Blaes, O. & Ionescu-Zanetti, C. 1998, MNRAS, 293, 1

Antonucci, R., Barvainis, R. & Alloin, D. 1990, ApJ, 353, 416

Antonucci, R., Geller, R., Goodrich, R.W. & Miller, J.S. 1996, ApJ, 472, 502

Antonucci, R.R.J. & Miller, J.S. 1985, ApJ, 297, 621

Awaki, H. 1997, in *Emission Lines in Active Galaxies: New Methods and Techniques*, eds. B.M. Peterson, F.-Z. Cheng & A.S. Wilson, ASP Conference Series, 113, 44

Awaki, H., Ueno, S., Koyama, K., Iwasawa, K. & Kuneida, H. 1997, Adv.Sp.R, 19, 95

Baker, J.C., 1997, MNRAS, 286, 23

Baker, J.C. & Hunstead, R.W. 1995, ApJL, 452, 95

Barvainis, R. 1992, ApJ, 400, 502

Barvainis, R. 1993, ApJ, 412, 513

Barvainis, R. 1990, ApJ, 353, 419

Barvainis, R., Antonucci, R. & Coleman, P. 1992, ApJ, 399, 19

Bechtold, J, Elvis, M., Fiore, F., Kuhn, O., Cutri, R.M., McDowell, J.C., Reike, M., Siemiginowska, A. & Wilkes, B.J. 1994, AJ, 108, 374

Becker, R.H., Gregg, M.D., Hook, I.M., McMahon, R.G., White, R.L. & Helfand, D.J. 1997, ApJL, 479, 93

Bergeron, J. & Kunth, D. 1984, MNRAS, 207, 263

Blanco, P., 1998, BAAS, 192, 3203

Blaes, O. & Agol, E. 1996, ApJL, 469, 41

Blundell, K.K. & Beasley, A.J. 1998, MNRAS, 299, 165

Boller, T., Brandt, W.N. & Fink, H. 1996, AA, 305, 53

Boroson, T.A. 1992, ApJL, 399, 15

Boroson, T.A. & Green, R.F. 1992, ApJS, 80, 109

Boroson, T.A., Persson, S.E. & Oke, J.B. 1985, ApJ, 293, 120

Boyle, B.J. & di Matteo, T. 1995, MNRAS, 277 L63

Boyle, B.J., Wilkes, B.J. & Elvis, M. 1997, MNRAS, 285, 511

Brissenden, R.J. 1989, PhD Thesis, Australian National University

Buehler, P., Courvoisier, T.,J-L., Staubert, R., Brunner, H. & Lamer, G. 1995, AA, 295, 309

Cappi, M., Matsuoka, M., Comastri, A., Brinkmann, W., Elvis, M., Palumbo, G.G.C. & Vignali, C. 1997, ApJ, 478, 492

Carleton, N.P., Elvis, M., Fabbiano, G., Willner, S.P., Lawrence, A. & Ward, M. 1987, ApJ, 318, 595

Catanese, M. *et al.* 1997, ApJL, 487, 143

Chini, R., Kreysa, E. & Biermann, P. L. 1989, AA, 219, 87

Chini, R., Kreysa, E. & Wargau, W.F., 1997, AA, 318, 15

Clavel, J., Wamsteker, W. & Glass, I.S. 1989, ApJ, 337, 236

Collin-Souffrin, S., Czerny, B., Dumont, A.-M., & Zycki, P.T. 1996, AA, 314, 393

Condon, J. J., Cotton, W. D., Greisen, E. W., Yin, Q. F., Perley, R. A., Taylor, G. B., & Broderick, J. J. 1998, AJ, 115, 1693

Courvoiser, T.,J-L. 1998, AA Reviews *in press*

Cutri, R.M., Wisniewski, W.Z., Reike, G.H. & Lebofsky, M.J. 1985, ApJ, 296, 423

Czerny, B. & Elvis, M. 1987, ApJ, 321, 305

de Bruyn, A.G. & Wilson, A.S. 1976, AA, 53, 93

Dunlop, J.S., Taylor, G.L., Hughes, D.H. & Robson 1993, MNRAS, 264, 455

Edelson, R.A. & Malkan, M.A. 1987, ApJ, 323, 516

Elvis, M., Fiore, F., Wilkes, B.J., McDowell, J. & Bechtold, J. 1994, ApJ, 422, 60

Elvis, M. S., Wilkes, B. J., McDowell, J. C., Green, R. F., Bechtold, J., Willner, S. P., Cutri, R., Oey, M, S., & Polomski, E. 1994, ApJS, 95, 1 (EWM94)

Fichtel, C.E., *et al.* 1994, ApJS, 94, 551

Fiore, F., Perola, G.C., Matsuoka, M., Yamauchi, M. & Prio, L. 1992, AA, 262, 37

Fiore, F., Elvis, M., McDowell, J.C., Siemiginowska, A. & Wilkes, B.J. 1994, ApJ, 431, 515

Fiore, F., Elvis, M., Siemiginowska, A., Wilkes, B.J., McDowell, J.C. & Mathur, S. 1995, ApJ, 449, 74

Fiore, F., Perola, G.C., Matsuoka, M., Yamauchi, M. & Piro, L. 1992, ApJ, 347, 171

Gear, W., Stevens, J.A., Hughes, D.H., Litchfiueld, S.J., Robson, E.I., Terasanta, H., Valtaoja, E., Steppe, H., Aller, M.F., & Aller, H.D. 1994, MNRAS, 267, 167

George, I.M. & Fabian, A.C. 1991, MNRAS, 249, 352

Giuliano, G., Dario, F. & Messetti, M. 1996, ApJ, 468, 475

Green, P.J., Schartel, N., Anderson, S.F., Hewett, P.C., Foltz, C.B., Brinkmann, W., Fink, H., Truemper, J. & Margon, B. 1995, ApJ, 450, 51

Green, P.J., Anderson, S.F. & Ward, M.J. 1992, MNRAS, 254, 30

Gregg, M.D., Becker, R.H., White, R.L., Helfand, D.J., McMahon, R. G. & Hook, I.M. 1996, AJ, 112, 407

Gondek, D., Zdziarski, A. A., Johnson, W. N., George, I. M., McNaron-Brown, K., Magdziarz, P., Smith, D. & Gruber, D. E. 1996, MNRAS, 282, 646

Guilbert, P.W. & Rees, M.J. 1988, MNRAS, 233, 475

Haardt, F., & Maraschi, L. 1993, ApJ, 413, 507

Haardt, F., & Maraschi, L. 1991, ApJ, 380, 51

Haardt, F., Maraschi, L. & Ghisellini, G. 1994, ApJ, 432, 95

Haas, M., Chini, R., Meisenheimer, K., Stickel, M., Lemke, D., Klaas, U. & Kreysa, E. 1998 ApJL, 503, 109

Halpern, J.P. 1984, ApJ, 281, 90

Hewett, P.C., Foltz, C.B., & Chaffee, F.H., 1995, AJ, 109, 1498

Hughes, D. H., Robson, E. I., Dunlop, J. S., Gear, W. K. 1993, MNRAS, 263, 607

Impey, D.D. & Neugebauer, G. 1988, AJ, 95 307

Jackson, N. & Browne, I.W.A. 1991, MNRAS, 250, 422

Joly, M. 1991, AA, 242, 49

Kim, D-W., & Elvis, M. 1998, ApJ, *submitted*

Kolman, M., Halpern, J.P., Shrader, C.R. & Filippenko, A.V. 1991, ApJ, 373, 57

Koratkar, A.P., Kinney, A.L. & Bohlin, R.C. 1992, ApJ, 400, 435

Koratkar, A.P., Antonucci, R.R.J., Goodrich, R.W., Bushouse, H. & Kinney, A.L. 1995, ApJ, 450, 501

Kriss, G.A. 1994, poster presented at the conference "The Analysis of Emission Lines: A Symposium in Honor of the 70th Birthdays of D.E. Osterbrock and M.J Seaton", eds. R. E. Williams & M. Livio, Baltimore: STScI.

Kriss, G.A. 1988, ApJ, 324, 809

Kuhn, O. 1996, PhD Thesis, Harvard University

Kuhn, O., Bechtold, J., Cutri, R. & Elvis, M. 1995, ApJ, 438, 643

Kukula, M.J., Pedlar, A., Baum, S.,A., & O'Dea, C.P. 1995, MNRAS, 276, 1262

Kukula, M. J., Dunlop, J. S., Hughes, D. H., & Rawlings, S. 1998, MNRAS, 297, 366

Kuraszkiewicz, J., Wilkes, B.J., Czerny, B. & Mathur, S. 1998, ApJ, *submitted*

La Franca, Franceschini, A., Cristiani, S. & Vio, R. 1995, AA, 299, 1995

Laor, A. 1990, MNRAS, 246, 369

Laor, A., Fiore, F., Elvis, M., Wilkes, B.J., McDowell, J.C. 1997, ApJ, 477, 93

Lawrence, A., Elvis, M. S., Wilkes, B. J., McHardy, I., Brandt, N. 1997, MNRAS, 285, 879

Lawrence, A., Rowan-Robinson, M., Efstathiou, A., Ward, M.,J., Elvis, M., Smith, M.G., Duncan, W.D. & Robson, E.I. 1991, MNRAS, 248, 91

Lawson, A.J. & Turner, M.J.L. 1997, MNRAS, 288, 920

Lonsdale, C.J., Smith, H.E. & Lonsdale, C.J. 1995, ApJ, 438, 632

Lightman, A. P. & White, T. R. 1988, ApJ, 335, 57

Mas-Hesse. J.M. 1992, AA, 253, 49

Masci, F.J., Drinkwater, M.J. & Webster, R.L. 1999 ApJ *in press* (Jan 10)

Masnou, J-L., Wilkes, B. J., Elvis, M., Arnaud, K. A. & McDowell, J. C. 1992, AA, 253, 35

Mathur, S., Elvis, M. & Wilkes, B. 1995, ApJ, 452, 230

McDowell, J.C., Elvis, M., Wilkes, B.J., Willner, S.P., Oey, M.S., Polomski, E., Bechtold, J. & Green, R.F. 1989, ApJL, 345, L13

McLeod, K.K., & Rieke, G.H. 1994a, ApJ, 420, 58

McLeod, K.K., & Rieke, G.H. 1994b, ApJ, 431, 137

Mushotzky, R. & Ferland, G.J. 1984, ApJ, 278, 558

Nandra, K., George, I. M., Mushotzky, R. F., Turner, T. J. & Yaqoob, T. 1997a ApJ, 477, 602

Nandra, K., George, I. M., Mushotzky, R. F., Turner, T. J. & Yaqoob, T. 1997b ApJ, 488, L91

Nandra, K. & Pounds, K.A. 1994, MNRAS, 268, 405

Neugebauer, G.A. 1996, BAAS, 28, 1307

Peacock, J.A. & Wall, J.V. 1982, MNRAS, 198, 843

Peterson, B.A., Foltz, C.B. & Byard, P.L. 1981, ApJ., 251, 4

Pier, E.A. & Krolik, J.H. 1993, ApJ, 418, 673

Pounds, K.A., Done, C. & Osborne, J.P. 1995, MNRAS, 277, L5

Pounds, K. A., Nandra, K, Stewart, G. C. George, I. M., & Fabian, A. C. 1990 Nature 344, 132

Puchnarewicz, E.M. *et al.* 1996, MNRAS, 281, 1243

Puchnarewicz, E.M. *et al.* 1992, MNRAS, 256, 589

Puchnarewicz, E.M., Mason, K.O., Siemiginowska, A. & Pounds, K.A. 1995, MNRAS, 276, 20

Reeves, J.N., Turner, M.J.L., Ohashi, T. & Kii, T. 1997, MNRAS, 292, 468

Reynolds, C.S. 1997, MNRAS, 286, 513

Roche, P.F., Whitmore, B., Aitken, D.K. & Phillips, M.M. 1984, MNRAS, 207, 35

Rowan-Robinson, M. 1995, MNRAS, 272, 737

Sanders, D., Phinney, E.S., Neugebauer, G., Soifer, B.T., & Matthews, K. 1989, ApJ, 347, 29

Schmidt, M. & Green, R. F. 1983, ApJ, 269, 352

Shastri, P., Wilkes, B.J., Elvis, M., & McDowell, J.C. 1993, ApJ, 410, 29

Shanks, T., Georgantopoulos, I., Stewart, G.C., Pounds, K.A., Boyle, B.J. & Griffiths, R.E. 1991, Nat., 353, 315

Shields, G.A., Wobus, L. & Husfeld, D. 1988, ApJ, 496, 743

Smith, D.A. & Done, C. 1996, MNRAS, 280, 355

Smith, H.E. & Spinrad, H. 1980, ApJ, 236, 419

Stocke, J.T., Morris, S.L., Gioia, I.M., Maccacaro, T., Schild, R., Wolter, A., Fleming, T.A., & Henry, P.J. 1991, ApJS, 76, 813

Sun, W-H. & Malkan, M.A. 1989, ApJ, 346, 68

Siemiginowska, A., Kuhn, O., Elvis, M., Fiore, F., McDowell, J. & Wilkes, B.J. 1995, ApJ, 454, 77

Tanaka, Y. *et al.* 1995, Nature, 375, 659

Tananbaum, H. *et al.* 1979, ApJL, 234, 9

Taylor, G.L., Dunlop, J.S., Hughes, D.H. & Robson, E.I., 1996, MNRAS, 283, 930

Treves, A., Bouchet, P, Chiappetti, L, Ciapi, A., Falomo, R., Maraschi, L. & Tanzi, E.G. 1988, ApJ, 330, 178

Tripp, T.M., Bechtold, J. & Green, R.F. 1994, ApJ, 433, 533

Tuerler, M., *et al.* 1998, AA, *in press*

Turner, T. J. & Pounds, K. A. 1989, MNRAS, 240,833

Turner, T.J., George, I.M., Nandra, K. & Mushotzky R.F. 1997a, ApJ, 488, 164

Turner, T.J., George, I.M., Nandra, K. & Mushotzky R.F. 1997b, ApJS, 113, 23

Ulvestad, J.S. 1982, ApJ, 259, 96

Ulvestad, J.S. & Wilson, A.S. 1984, ApJ, 278, 544

Wandel, A. & Boller, T. 1998, AA, 331, 884

Webster, R.L., Francis, P.J., Peterson, B.A., Drinkwater, M.J. & Mascl, F.J. 1995, Nature, 375, 469

Wilkes, B. J. & Elvis, M. S. 1987 ApJ, 323, 243

Wilkes, B.J., Kuraszkiewicz, J., Green, P., Mathur, S. & McDowell, J.C. 1999, ApJ, 512 *in press* (Mar 1)

Wilkes, B.J., Mathur, S., Fiore, F. & Antonelli, A. 1998 in **Structure and Kinematics of Quasar Broad Line Regions** eds. C.M. Gaskell, W.N. Brandt, D. Dultzin-Hacyan, M. Eracleous & M. Dietrich, ASP Conference Series, *in press*

Wilkes, B.J., Tananbaum, H., Avni, Y., Worrall, D.M., Oey, M.S. & Flanagan, J. 1994, ApJS, 92, 53

Williams *et al.* 1992, ApJ, 389, 157

Wills, B.J. & Browne, I.W.A. 1986, ApJ, 302, 56

Worrall, D.M., Tananbaum, H., Giommi, P. & Zamorani, G. 1987, ApJ, 313, 596

Yaqoob, T., Warwick, R.S., Makin, F., Otani, C., Sokoloski, J.L., Bond, I.A. & Yamauchi, M. 1993, MNRAS, 262, 435

Yuan, W., Siebert, J. & Brinkmann, W. 1998, AA, 334, 498

Zamorani, G. *et al.* 1981, ApJ, 245, 357

Zdziarski, A.A., Fabian, A.C., Nandra, K., Celotti, A., Rees, M.J., Done, C., Coppi, P.S. & Madejski, G.M. 1994, MNRAS, 269, L55

Zdziarski, A.A., Gierlinski, M., Gondek, D. & Magdziarz, P. 1996, AAS, 120, 553

Zheng, W., Kriss, G. A., Telfer, R. C., Grimes, J. P. & Davidsen, A. F. 1997, ApJ, 475, 469

Zheng, W. & Malkan, M.A. 1993, ApJ, 415, 517

Zweerink, J.A. *et al.* 1997, ApJL, 490, 141